

Scaling of the Reduced Energy Spectrum of Random Matrix Ensemble

Wen-Jia Rao* and M. N. Chen
School of Science, Hangzhou Dianzi University, Hangzhou 310027, China.
(Dated: March 2, 2022)

Recent works found the higher order level spacings and non-overlapping gap ratios in a random matrix ensemble follow the same form of rescaling for their distributions, for which a consistent explanation is given in this work. The key we find is the reduced energy spectrum $\{E_i^{(n)}\}$ constructed by picking one level from every n levels from the original spectrum $\{E_i\}$. It's shown $\{E_i^{(n)}\}$ follow the same form of distribution as $\{E_i\}$ with a rescaled parameter $\gamma = \frac{n(n+1)}{2}\beta + n - 1$. Notably, the nearest level spacing and gap ratio in $\{E_i^{(n)}\}$ correspond to the n -th order level spacing and non-overlapping gap ratio in $\{E_i\}$, hence explaining their distributions simultaneously. Numerical evidences are provided from modelling random matrix and random spin chain.

PACS numbers: 84.35.+i, 71.55.Jv, 75.10.Pq, 64.60.aq

I. INTRODUCTION

Random matrix theory (RMT) is a powerful mathematical tool for studying complex quantum systems, it describes the universal properties of random matrix that are determined only by the system's symmetry while independent of microscopic details. Specifically, Gaussian orthogonal ensemble (GOE) describes systems with time reversal invariance; Gaussian unitary ensemble (GUE) corresponds to systems without time reversal symmetry but conserves spin rotational invariance; and Gaussian symplectic ensemble (GSE) represents time reversal invariant systems without spin rotational symmetry, e.g. the ones with Rashba spin-orbital coupling. For this reason, RMT has been applied to various fields ranging from disordered nuclei to isolated quantum many-body system¹⁻³.

The distribution of nearest level spacings, i.e. the gaps between neighboring energy levels $\{s_i = E_{i+1} - E_i\}$, is by far the most widely-used statistical quantity since it measures the strength of level repulsion. It is well established that $\{s_i\}$ follows a Wigner-Dyson distribution in a thermal phase with level repulsion, while a Poisson distribution is expected for localized phase with independent spectrum^{4,5}. However, to obtain a universal level spacing distribution $P(s)$, an unfolding procedure is required to erase the model-dependent information about local density of states (DOS). This procedure is, however, cumbersome and non-unique and suffers from subtle ambiguity raised by concrete unfolding strategy⁶.

To overcome this problem, Oganesyan and Huse⁷ introduced the distribution $P(r)$ for the ratios between consecutive gaps $\{r_i = s_{i+1}/s_i\}$, whose analytical form was later derived by Atas *et al.*⁸. Although $P(r)$ does not reveal the strength of level repulsion in a direct way, it is independent of local DOS, hence requires no unfolding procedure. For this reason, the gap ratio has found various applications, and in many cases gives better results than level spacing⁹⁻¹⁴.

Both the nearest level spacing and gap ratio measure short-range level correlations, and have been generalized to higher order to describe level correlations on longer range¹⁵⁻²². The n -th order level spacing is defined as $\{s_i^{(n)} = E_{i+n} - E_i\}$, its distribution is proved in Ref. [15] to bear the same form as Wigner-Dyson distribution (see Eq. (3) in Sec. II) with a

rescaled parameter

$$\gamma = \frac{n(n+1)}{2}\beta + n - 1, \quad (1)$$

where $\beta = 1, 2, 4$ stands for GOE, GUE, GSE respectively. On the other hand, a kind of higher order generalization of gap ratio – so called non-overlapping gap ratio – has also been studied, which is defined as $\{r_i^{(n)} = s_{i+n}/s_i^{(n)}\}$. Ref. [19] provides compelling numerical evidence that $P(r^{(n)})$ follows the same form with $P(r)$ with a rescaled parameter that is identical to the one in Eq. (1). This strongly hints a homogeneous relation between the higher-order level spacing and non-overlapping gap ratio, but an explanation is lacking, which motivates current work.

In this work, we find that the behaviors of higher order level spacing and non-overlapping gap ratios can be explained simultaneously by studying the reduced energy spectrum $\{E_i^{(n)} \equiv E_{in}\}$, i.e. the spectrum constructed by picking one level from every n levels of the original spectrum $\{E_i\}$. It is shown the distribution of $\{E_i^{(n)}\}$ bears the same form as $\{E_i\}$ with a rescaled parameter expressed in Eq. (1). Notably, the nearest level spacing and gap ratio in $\{E_i^{(n)}\}$ corresponds to the n -th order level spacing and non-overlapping gap ratio in $\{E_i\}$, hence explaining their distributions at the same time.

This paper is organized as follows. In Sec. II we summarize the known formulas regarding the higher-order level spacings and gap ratios, which will be used for later numerical fittings. In Sec. III we give a formal definition of the reduced energy spectrum, and provides compelling evidence for the behavior of its distribution. In Sec. IV we provide numerical fittings for the level spacing and gap ratio distributions in the reduced energy spectrum. Conclusion and discussion come in Sec. V.

II. SUMMARY OF KNOWN RESULTS

The starting point to study the spectral statistics in Gaussian ensembles is the distribution of energy levels, whose form is

$$P(\beta, \{E_i\}) = C \prod_{i < j} |E_i - E_j|^\beta e^{-A \sum_{i=1}^N E_i^2}, \quad (2)$$

where $\beta = 1, 2, 4$ for GOE,GUE,GSE respectively, C and A are coefficients correlated by the normalization condition $\int \prod_i dE_i P(\beta, \{E_i\}) = 1$. From this distribution, we can in principle calculate any statistical quantity we want, in particular the distribution of nearest level spacing and gap ratio. The general distributions for them in large dimension N are complicated, while for most practical purpose it is sufficient to adopt the so-called Wigner surmise that deals with smallest matrix that holds the quantity of interest. For example, to study nearest level spacing it's sufficient to consider a 2×2 matrix, which gives the famous Wigner-Dyson distribution⁵

$$P(\beta, s) = C(\beta) s^\beta e^{-A(\beta)s^2} \quad (3)$$

the coefficients $C(\beta), A(\beta)$ are determined by the normalization conditions

$$\int_0^\infty P(\beta, s) ds = 1, \int_0^\infty s P(\beta, s) ds = 1, \quad (4)$$

for which we obtain

$$A(\beta) = \left(\frac{\Gamma(\beta/2 + 1)}{\Gamma(\beta/2 + 1/2)} \right)^2, C(\beta) = \frac{2\Gamma^{n+1}(\beta/2 + 1)}{\Gamma^{n+2}(\beta/2 + 1/2)}, \quad (5)$$

where $\Gamma(z) = \int_0^\infty t^{z-1} e^{-t} dt$ is the Gamma function.

As to study the distribution of nearest gap ratios $\{r_i = s_{i+1}/s_i\}$, a Wigner like surmise is applicable by studying 3×3 matrix⁸, which gives

$$P(\beta, r) = \frac{1}{Z_\beta} \frac{(r + r^2)^\beta}{(1 + r + r^2)^{1+3\beta/2}} \quad (6)$$

where Z_β is the normalization factor determined by requiring $\int_0^\infty P(\beta, r) dr = 1$. It is crucial to note that the derivation for Eq. (3) and Eq. (6) is purely mathematical, that is, applicable for arbitrary positive number β .

For the higher order level spacings $\{s_i^{(n)} = E_{i+n} - E_i\}$, it is proved in Ref. [15] using a Wigner-like surmise that deals with $(n+1) \times (n+1)$ matrix, and the result shows they follow a generalized Wigner-Dyson distribution that bears the same form as Eq. (3) with the parameter β rescaled to γ as expressed in Eq. (1).

On the other hand, higher order gap ratios come in two different ways, i.e. the “overlapping”¹⁸ and “non-overlapping”¹⁹ ways. In the former case we are dealing with

$$\tilde{r}_i^{(n)} = \frac{E_{i+n} - E_i}{E_{i+n-1} - E_{i-1}} = \frac{s_{i+n} + s_{i+n-1} + \dots + s_{i+1}}{s_{i+n-1} + s_{i+n-2} + \dots + s_i}, \quad (7)$$

which is termed “overlapping” gap ratio since there are shared spacings between the numerator and denominator. While the n -th order “non-overlapping” gap ratio is defined as

$$r_i^{(n)} = \frac{E_{i+2n} - E_{i+n}}{E_{i+n} - E_i} = \frac{s_{i+2n} + s_{i+2n-1} + \dots + s_{i+n+1}}{s_{i+n} + s_{i+n-1} + \dots + s_i}. \quad (8)$$

Both these two generalizations reduce to the nearest gap ratio when $n = 1$, but they are very different when studying their

distributions using Wigner surmise: for non-overlapping ratio $r^{(n)}$, the smallest matrix dimension is $(2n+1) \times (2n+1)$; while it is $(n+2) \times (2+2)$ for overlapping ratios. Naively, it's expected that $P(\tilde{r}^{(n)})$ is more complicated due to the overlapping spacings. Indeed, the analytical form of $P(\tilde{r}^{(2)})$ was worked out in Ref. [18] and the result is quite involving. For the non-overlapping ratios, Ref. [19] provides compelling numerical evidence that $P(r^{(n)})$ bears the same form as $P(r)$ with the same rescaling parameter as higher order level spacing, that is, Eq. (1).

In summary, we have

$$P(\beta, s^{(n)}) = P(\gamma, s), \quad (9)$$

$$P(\beta, r^{(n)}) = P(\gamma, r) \quad (10)$$

where γ is expressed in Eq. (1).

III. REDUCED ENERGY SPECTRUM

The identical rescaling for higher level spacing and non-overlapping gap ratio strongly hints a homogeneous relation between $P(s^{(n)})$ and $P(r^{(n)})$, but a formal mathematical relation is difficult to obtain. Instead, we can relate them by constructing a so-called reduced energy spectrum. Formally, a reduced energy spectrum $\{E_i^{(n)} \equiv E_{in}\}$ is constructed by picking one level from every n levels of the original spectrum $\{E_i\}$, hence the dimension of $\{E_i^{(n)}\}$ is $\lceil \frac{N}{n} \rceil$. By this construction, the density of states for $\{E_i\}$ and $\{E_i^{(n)}\}$ are identical, and the probability distribution of $\{E_i^{(n)}\}$ is

$$P(\{E_i^{(n)}\}) = \prod_i \int_{E_{in}}^{E_{(i+1)n}} \prod_{j=i+1}^{(i+1)n-1} dE_j P(\beta, \{E_i\}). \quad (11)$$

The interest of this construction is, the nearest level spacing and gap ratio in $\{E_i^{(n)}\}$ correspond to the n -th order level spacing and non-overlapping gap ratio in $\{E_i\}$. As mentioned before, the derivation for the distributions in Eq. (3) and Eq. (6) works for arbitrary positive β , therefore, if the distribution of $P(\{E_i^{(n)}\})$ (to leading order) bear the same form as $P(\{E_i\})$ with the rescaled parameter γ as Eq. (1), that is,

$$P(\{E_i^{(n)}\}) \sim \prod_{i < j} |E_i^{(n)} - E_j^{(n)}|^\gamma e^{-A' \sum_{i=1}^{N/n} (E_i^{(n)})^2}, \quad (12)$$

then the behavior of the $P(s^{(n)})$ and $P(r^{(n)})$ in Eq. (9) and Eq. (10) can be explained at the same time. It is then our purpose to verify this formula. Firstly, the constant A' is not important since it is only an overall decaying parameter, whose value can be tuned with global rescaling of the energy levels without affecting the distribution of level spacing or gap ratio.

Therefore, we will focus on the parameter γ that controls the strength of level repulsion.

A formal derivation from Eq. (11) to Eq. (12) is mathematically challenging. It is not our purpose to give a general proof for arbitrary dimension N , instead, we will prove Eq. (12) to hold in the sense of Wigner surmise. Recall that Wigner surmise works for the smallest matrix that holds the quantity we are interested in, therefore, to study the nearest level spacing (gap ratio) in $\{E_i^{(n)}\}$, it's sufficient to consider the cases with only 2 (3) levels, which we will study separately in the following.

We start with the case that $\{E_i^{(n)}\}$ has only two levels, the rescaling Eq. (12) becomes

$$I(E_0, E_n) = \int_{E_0}^{E_n} \prod_{i=1}^{n-1} dE_i P(\beta, \{E_i\}) \quad (13)$$

$$\sim |E_0 - E_n|^\gamma e^{-A'(E_0^2 + E_n^2)}.$$

Denote $E_0 = R \cos \theta$ and $E_n = R \sin \theta$, and keeping R constant, we have

$$\log I(\theta) = \gamma \log |\cos \theta - \sin \theta| + \text{const.} \quad (14)$$

We then provide a numerical check for this formula.

Without loss of generality, we take $A = 1$ and $R = 1$, and randomly generate 200 sets of θ in the range $[0, 2\pi)$. We then numerically calculate $\log I(\theta)$ and $\log |\cos \theta - \sin \theta|$, and collect the results for $n = 2, 3, 4$ in $\beta = 1, 2, 3, 4$ cases, the are presented in Fig. 1. As can be seen, the $\log I(\theta)$ and $\log |\cos \theta - \sin \theta|$ shows a perfect linear dependence in all the cases, where the fitted γ are displayed in the figure legends. All the fitted values of γ are quite close to the expected ones in Eq. (1), with the largest deviation being only 3.15%, as summarized in Table I. Actually the relation Eq. (14) not restricted to the Gaussian ensembles with $\beta = 1, 2, 4$ but valid for general positive β , for which we present the $\beta = 3$ case as an example.

Next, to study the gap ratio distribution, we consider the case that $\{E_i^{(n)}\}$ has three levels, when the rescaling Eq. (12) becomes

$$Q(E_0, E_n, E_{2n}) \quad (15)$$

$$\equiv \int_{E_0}^{E_n} \prod_{i=1}^{n-1} dE_i \int_{E_n}^{E_{2n}} \prod_{j=n+1}^{2n-1} dE_j P(\beta, \{E_i\})$$

$$\sim |E_0 - E_n|^\gamma |E_n - E_{2n}|^\gamma |E_0 - E_{2n}|^\gamma e^{-A'(E_0^2 + E_n^2 + E_{2n}^2)}.$$

With the transformation to spherical coordinates

$$E_0 = R \sin \theta \cos \varphi, E_n = R \sin \theta \sin \varphi, E_{2n} = R \cos \theta \quad (16)$$

and keeping R constant, we will have

$$\log Q(r, \theta, \varphi) = \gamma \log G(\theta, \varphi) + \text{const.} \quad (17)$$

where

$$G(\theta, \varphi) = |(\sin \theta \cos \varphi - \sin \theta \sin \varphi) \times (\sin \theta \cos \varphi - \cos \theta) \times (\sin \theta \sin \varphi - \cos \theta)|. \quad (18)$$

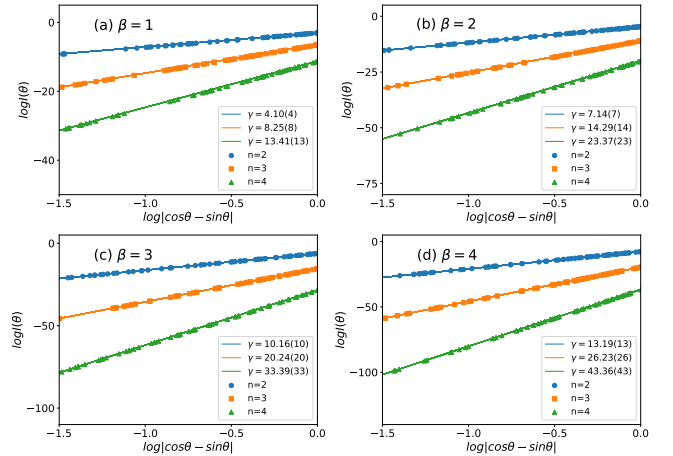


FIG. 1. The fitting of Eq. (14) for $\beta = 1, 2, 3, 4$ with $n = 2, 3, 4$. The fitted slopes are shown in the figure legends, where the numbers in the bracket are the expected values according to Eq. (1).

We then provide numerical checks, where we fix $R = 1$ and $A = 1$ as before. We randomly generate 200 sets of (θ, φ) and numerically determine $\log Q(\theta, \varphi) \equiv \log Q(1, \theta, \varphi)$ and $\log G(\theta, \varphi)$, the results are displayed in Fig. 2. Again, we show the results for $n = 2, 3, 4$ in $\beta = 1, 2, 3, 4$ cases. As can be seen, the linear dependence between $\log Q(\theta, \varphi)$ and $\log G(\theta, \varphi)$ is still good enough in all cases, although the deviations are slightly larger than that in Fig. 1, especially for $n \geq 3$ cases. This is partially due to the error raised by numerical integrals, where we adopted Monte-Carlo simulations to calculate the integral for these cases.

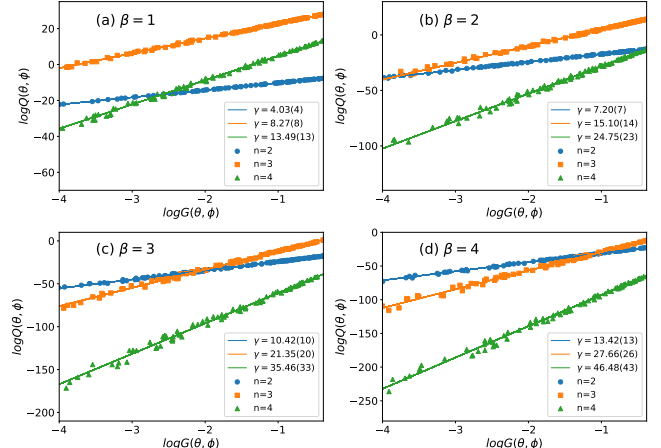


FIG. 2. The fitting of Eq. (17) for $\beta = 1, 2, 3, 4$ with $n = 2, 3, 4$. The fitted γ values are shown in the figure legends, with the expected values according to Eq. (1) in the brackets. In general, the deviations are slightly larger than those in Fig. 1.

For convenience, we list the expected and numerical values for γ and their relative deviations in Table I, where γ_e refers to the expected value according to Eq. (1), $\gamma_{\text{num.}}^{(1)}$ and $\gamma_{\text{num.}}^{(2)}$ are the values fitted from Eq. (14) and Eq. (17) respectively.

β	n	γ_e	$\gamma_{\text{num.}}^{(1)}$	error ⁽¹⁾	$\gamma_{\text{num.}}^{(2)}$	error ⁽²⁾
1	2	4	4.10	2.50%	4.03	0.75%
	3	8	8.25	3.13%	8.27	3.38%
	4	13	13.41	3.15%	13.49	3.77%
2	2	7	7.14	2.00%	7.20	2.86%
	3	14	14.29	2.07%	15.10	7.86%
	4	23	23.37	1.61%	24.75	7.29%
3	2	10	10.16	1.60%	10.42	4.20%
	3	20	20.24	1.20%	21.35	6.75%
	4	33	33.39	1.18%	35.46	7.45%
4	2	13	13.19	1.46%	13.42	3.23%
	3	26	26.23	0.88%	27.66	6.38%
	4	43	43.36	0.84%	46.48	8.09%

TABLE I. The values of γ with different β and order n , where v_e is the expected value according to Eq. (1). $\gamma_{\text{num.}}^{(1)}$ and $\gamma_{\text{num.}}^{(2)}$ are the values fitted from Eq. (14) and Eq. (17), their relative errors with respect to v_e are denoted by error⁽¹⁾ and error⁽²⁾ respectively.

Up to now, we have verified the distribution of $\{E_i^{(n)}\}$ in the cases with two and three levels, which is sufficient to study the nearest level spacing and gap ratio respectively using Wigner surmise. The verification in more general cases can be done in a similar manner, which is unnecessary for the purpose of current work, hence will not be done here.

IV. NUMERICAL SIMULATIONS

The numerical results in previous section provide strong evidence to support the distribution of reduced energy spectrum $\{E_i^{(n)}\}$ to follow the form in Eq. (12), hence it's expected the nearest level spacing and gap ratio will follow the same distribution as the n -th order level spacing and non-overlapping ratio in $\{E_i\}$, whose forms are expressed in Eq. (9) and Eq. (10). In this section we provide numerical simulations for the nearest level spacing and gap ratio of $\{E_i^{(n)}\}$ from modelling random matrix with large dimension in GOE, GUE and GSE.

Before that, there is a technical issue worth pointing out. That is, the nearest level spacing in $\{E_i^{(n)}\}$ is actually $E_{i+1}^{(n)} - E_i^{(n)} = E_{(i+1)n} - E_{in}$, therefore the number of them is $\left[\frac{N}{n}\right] - 1$; while in original energy spectrum $\{E_i\}$, the n -th order level spacing is $E_{i+n} - E_i$ with total number $N - n$; hence the mapping does not strictly hold, the same thing happens for gap ratios. However, since the distribution is extracted from a large number of level spacings (gap ratios), it's natural to suspect the difference is negligible when the number of samples and matrix dimension are large, which we will soon justify.

The matrix in GOE is constructed by

$$M_o = x + x^T \quad (19)$$

where x is a $N \times N$ real matrix with random elements drawn from a Gaussian distribution with mean $\mu = 0$ and standard

deviation $\sigma = 1$. The matrix in GUE is constructed by

$$M_u = x + x^\dagger \quad (20)$$

where x is a $N \times N$ complex matrix with both real and image part drawn from the same Gaussian distribution as in GOE case. As for GSE, the representative matrix is

$$M_s = x + x^\dagger - J(x + x^\dagger)J^\dagger \quad (21)$$

where $J = (-i\sigma_y) \otimes I_n$ with σ_y , I_n being the Pauli matrix and $n \times n$ identity matrix respectively, and x is a $2N \times 2N$ complex random matrix. The eigenvalue spectrum of M_s has two-fold Kramers degeneracy, which we manually remove when collecting the energy spectrum.

The distributions of nearest level spacings and gap ratios in the reduced energy spectrum $\{E_i^{(n)}\}$ in these three ensembles with $n = 2, 3, 4$ are summarized in Fig. 3, where the number of samples is 500, and the dimension of original energy spectrum is $N = 1000$. The data for level spacings are collected from the middle half levels of $\{E_i^{(n)}\}$ where the density of states is almost uniform, while that for gap ratio are taken from the whole spectrum. As can be seen, the fittings are perfectly consistent with the predictions in Eq. (9) and Eq. (10), confirming the correspondence between the nearest level spacing (gap ratio) in $\{E_i^{(n)}\}$ with the n -th order level spacing (non-overlapping gap ratio) in $\{E_i\}$.

We also study the relatively trivial case of Poisson ensemble. It is proved in Ref. [15] the n -th order level spacing in Poisson ensemble follows the generalized semi-Poisson distribution

$$P_n(s) = \frac{n^n}{\Gamma(n)} s^{n-1} e^{-ns} \quad (22)$$

which reduces to the conventional Poisson distribution when $n = 1$. For the n -th order non-overlapping gap ratios, we find they follow

$$P(r, n) = \frac{r^{n-1}}{(1+r^2)^{2n}} \quad (23)$$

which reduces to the results derived in Ref. [8] when $n = 1$.

With similarly constructed reduced energy spectrum, we verified the correspondence of nearest level spacing (gap ratio) with n -th order level spacing (non-overlapping gap ratio). The numerical results are given in Fig. 4, as can be seen, the fittings are perfect.

To further test above conclusions in a real physical system, we perform simulations in random spin chain, which is the canonical model to study many-body localization²³. The Hamiltonian reads

$$H = \sum_{i=1}^L \mathbf{S}_i \cdot \mathbf{S}_{i+1} + \sum_{i=1}^L \sum_{\alpha=x,y,z} h^\alpha \varepsilon_i^\alpha S_i^\alpha, \quad (24)$$

where \mathbf{S}_i is spin-1/2 operator. The anti-ferromagnetic coupling strength is set to be unity, and ε_i^α 's are random numbers within range $[-1, 1]$. The h^α is referred as randomness

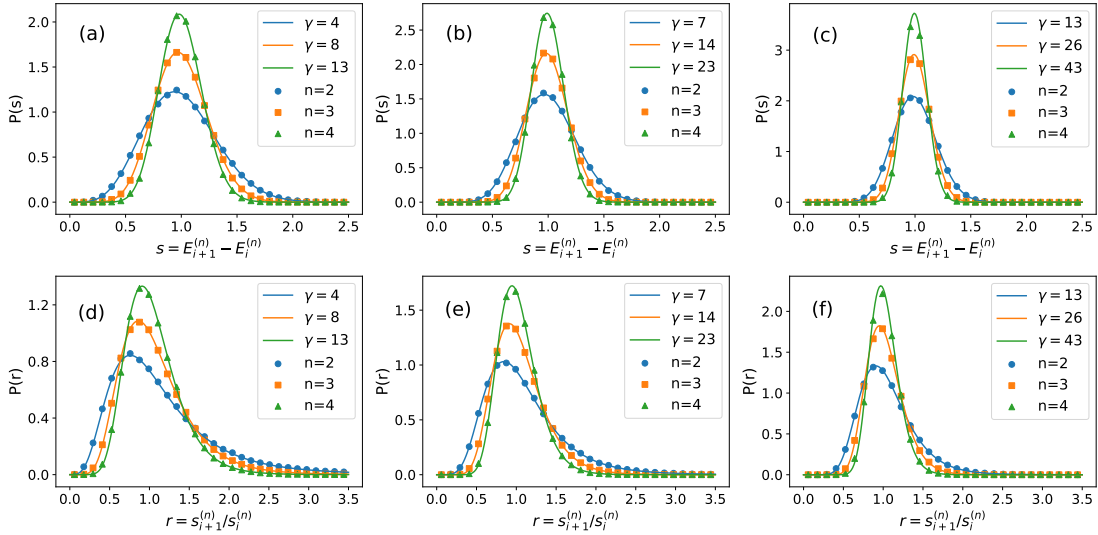


FIG. 3. Distribution of nearest level spacing and gap ratio in the reduced energy spectrum $\{E_i^{(n)}\}$ for matrix in GOE((a) and (d)), GUE((b) and (e)) and GSE((c) and (f)). The reference distribution curves in (a),(b),(c) are the ones in Eq. (9), and those in (d),(e),(f) are from Eq. (10), with parameter γ calculated from Eq. (1). The data for level spacings are collected from the middle half of the spectrum where DOS is almost uniform, and those for gap ratios are taken from the whole reduced energy spectrum.

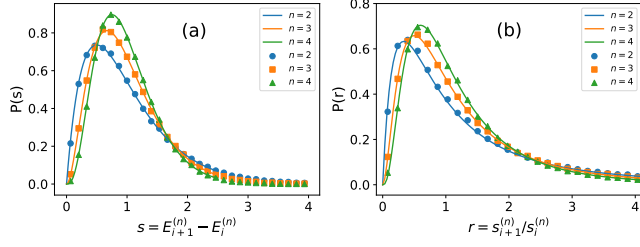


FIG. 4. Distribution of (a) nearest level spacing and (b) gap ratio in the reduced energy spectrum of Poisson ensemble, where the dots denote the numerical data from $\{E_i^{(n)}\}$, and the reference distribution curves corresponding to the ones in Ref. (22) and Ref. (23) with index n for level spacing and gap ratio respectively.

strength. We consider two choices of h^α : (i) $h^x = h^z = h \neq 0$ and $h^y = 0$, when the model is orthogonal and belongs to GOE; (ii) $h^x = h^y = h^z = h \neq 0$, when the model is unitary and belongs to GUE. This model undergoes a thermal-MBL transition at roughly $h_c \simeq 3$ (2.5) in the orthogonal (unitary) case, where the level spacing distribution evolves from GOE (GUE) to Poisson^{24,25}.

We choose a $L = 12$ system to present a numerical simulation, and prepare 500 samples of energy spectrum at $h = 1$ for both the orthogonal and unitary model, which represents GOE and GUE respectively. For each energy spectrum, we construct the reduced energy spectrum $\{E_i^{(n)}\}$ with $n = 2, 3, 4$ and collect the corresponding nearest level spacings and gap ratios, the results are displayed in Fig. 5. As can be seen, the fittings are quite satisfactory. The fittings for level spacings have slightly larger deviations, which is due to the non-

uniformity of local DOS; while those for gap ratios are perfect since it's independent of DOS. Therefore, the gap ratio is indeed a better choice to study spectral statistics.

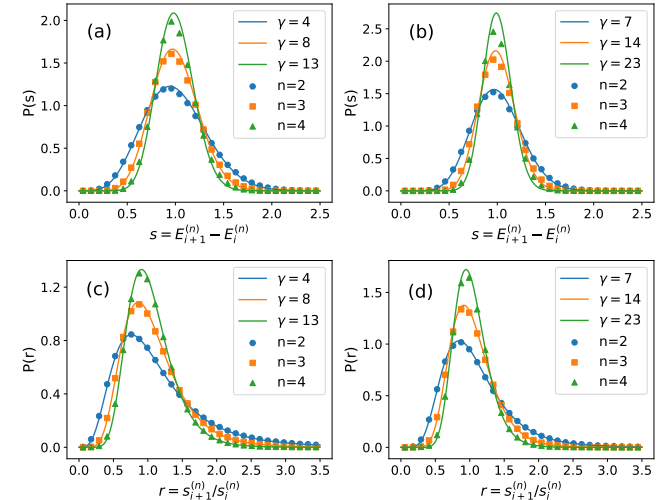


FIG. 5. Distribution of nearest level spacings of the reduced energy spectrum $\{E_i^{(n)}\}$ in (a) orthogonal and (b) unitary model of the Hamiltonian Eq. (24), the corresponding distributions for gap ratios are in (c) and (d) respectively. The reference distribution curves in (a),(b) are the ones in Eq. (9), and those in (c),(d) are from Eq. (10), with the parameter γ calculated from Eq. (1).

V. CONCLUSION AND DISCUSSION

We studied the reduced energy spectrum $\{E_i^{(n)}\}$, constructed by picking one levels from every n level in original spectrum $\{E_i\}$. It is verified the distribution of $\{E_i^{(n)}\}$ bears the same form as $\{E_i\}$, with the level repulsion parameter rescaled to $\gamma = \frac{n(n+1)}{2}\beta + n - 1$. It's then demonstrated the nearest level spacing (gap ratio) in $\{E_i^{(n)}\}$ correspond to the n -th order level spacing (non-overlapping gap ratio) in $\{E_i\}$, therefore explaining the distributions of the latter found recently in Ref. [15] (Ref. [19]). We also confirmed such correspondence for level spacings and gap ratios in the Poisson ensemble, and discovered the distribution for n -th order non-overlapping gap ratios, as expressed in Eq. (23).

The rescaling behavior from $\{E_i\}$ to $\{E_i^{(n)}\}$ is purely mathematical, that is, hold for arbitrary positive β , hence can find potential applications in models that goes beyond standard Gaussian ensembles. For example, the floquet or non-Hermitian system that holds complex energy spectrum²⁶. We also note the $\beta = 3$ behavior for level spacing has been found in a 2D non-Hermitian lattice²⁷.

Though the construction of reduced energy spectrum is artificial, it reveals a rich set of structures in the energy spectrum of random matrix. That is, a hierarchy of spectrums can emerge from single ensemble of energy spectrum, which can be viewed as a discretized subset of so-called Gaussian β ensemble of random matrix that has a continuous parameter $\beta \in (0, \infty)^{28}$. The modelling matrix that holds the distribution according to β ensemble has been known for a while²⁹, hence the “parent matrix” of the reduced energy spectrum in this work can be constructed accordingly. Therefore, an interesting and natural question is whether this “parent matrix” describes real quantum system, and what's the property of such a system if it does. In particular, our results strongly suggests that $\{E_i^{(2)}\}$ in GOE has the same structure as $\{E_i\}$ in GSE, which suggests the “parent Hamiltonian” of the former secretly belongs to GSE. Requests for such problems are intriguing directions for future study.

ACKNOWLEDGEMENTS

This work is supported by the National Natural Science Foundation of China through Grant No.11904069 and No.11847005 and No.11804070.

-
- * Corresponding author: wjrao@hdu.edu.cn
- ¹ C. E. Porter, Statistical Theories of Spectra: Fluctuations (Academic Press, New York), 1965.
- ² T. A. Brody et al., Rev. Mod. **53**, 385 (1981).
- ³ T. Guhr, A. Muller-Groeling, H. A. Weidenmuller, Phys. Rep. **299**, 189 (1998).
- ⁴ M. L. Mehta, Random Matrix Theory, Springer, New York (1990).
- ⁵ F. Haake, Quantum Signatures of Chaos (Springer 2001).
- ⁶ J. M. G. Gomez, R. A. Molina, A. Relano, and J. Retamosa, Phys. Rev. E **66**, 036209 (2002).
- ⁷ V. Oganesyan and D. A. Huse, Phys. Rev. B **75**, 155111 (2007).
- ⁸ Y. Y. Atas, E. Bogomolny, O. Giraud, and G. Roux, Phys. Rev. Lett. **110**, 084101 (2013).
- ⁹ V. Oganesyan, A. Pal, D. A. Huse, Phys. Rev. B **80**, 115104 (2009).
- ¹⁰ A. Pal, D. A. Huse, Phys. Rev. B **82**, 174411 (2010).
- ¹¹ S. Iyer, V. Oganesyan, G. Refael, D. A. Huse, Phys. Rev. B **87**, 134202 (2013).
- ¹² X. Li, S. Ganeshan, J. H. Pixley, and S. Das Sarma, Phys. Rev. Lett. **115**, 186601 (2015).
- ¹³ David J. Luitz, Nicolas Laflorencie, and Fabien Alet, Phys. Rev. B **91**, 081103(R) (2015).
- ¹⁴ A. Sarkar, M. Kothiyal, and S. Kumar, Phys. Rev. E **101**, 012216 (2020).
- ¹⁵ W.-J. Rao, arXiv:2005.08721.
- ¹⁶ R. Kausar, W.-J. Rao, and X. Wan, arXiv:2005.00721.
- ¹⁷ A. Y. Abul-Magd and M. H. Simbel, Phys. Rev. E **60**, 5371 (1999).
- ¹⁸ Y. Y. Atas, E. Bogomolny, O. Giraud, P. Vivo, and E. Vivo, J. Phys. A: Math. Theor. **46**, 355204 (2013).
- ¹⁹ S. H. Tekur, U. T. Bhosale, and M. S. Santhanam, Phys. Rev. B **98**, 104305 (2018).
- ²⁰ S. H. Tekur, S. Kumar and M. S. Santhanam, Phys. Rev. E, **97**, 062212 (2018).
- ²¹ P. J. Forrester, Comm. Math. Phys. **285**, 653 (2009).
- ²² P. Rao, M. Vyasa, and N. D. Chavda, arXiv:1912.05664v1.
- ²³ F. Alet and N. Laflorencie, C. R. Physique **19**, 498-525 (2018).
- ²⁴ N. Regnault and R. Nandkishore, Phys. Rev. B **93**, 104203 (2016).
- ²⁵ S. D. Geraedts, R. Nandkishore, and N. Regnault, Phys. Rev. B **93**, 174202 (2016).
- ²⁶ L. Sa, P. Ribeiro, and T. Prosen, Phys. Rev. X **10**, 021019 (2020).
- ²⁷ A. F. Tzortzakakis, K. G. Makris, and E. N. Economou, Phys. Rev. B **101**, 014202 (2020).
- ²⁸ W. Buijsman, V. Cheianov, and V. Gritsev, Phys. Rev. Lett. **122**, 180601 (2019).
- ²⁹ I. Dumitriu and A. Edelman, J. Math. Phys. **43**, 5830 (2002).